JOURNAL OF SOLID STATE CHEMISTRY 41, 1–22 (1982)

Mössbauer ^{57}Fe Isomer Shift as a Measure of Valence in Mixed-Valence Iron Sulfides

JOHN B. GOODENOUGH

Inorganic Chemistry Laboratory, South Parks Road, Oxford, OX1 3QR, England

AND G. A. FATSEAS

Laboratoire de Chimie des Solides, associe au CNRS, (L.A. No. 279), 2 rue de la Houssiniere, (F)-44072 Nantes Cedex, France

Received June 2, 1981

An empirical formula relating the room-temperature isomer shift δ for high-spin iron in sulfur coordination to the effective iron valence $\langle m+ \rangle$, of the form $\delta = A - B\langle m+ \rangle$, has been refined for tetrahedral coordination and modified by an inclusion of orbital degeneracy into the definition of $\langle m+ \rangle$; it has also been extended to include octahedral coordination by adding 0.17 mm/sec to A. For a given $\langle m+ \rangle$, the I.S. is shown to be sensitive to nearest-neighbor anion coordination, but much less sensitive than the hyperfine field to the competitive bonding with these anions. However, the sign of the deviation from the empirical line indicates the direction of any net superexchange charge transfer to or from the iron atom. The utility of the relationship is illustrated by application to a wide range of problems.

Introduction

In a previous paper (*1*), we discussed the Mössbauer ^{57}Fe spectra exhibited by iron ions having a divalent formal valence and hence a "ferrous character." In that paper we stressed how the isomer shift (I.S.) provides a guide not only to the existence of high-spin versus low-spin states, but also to localized versus itinerant electrons and to a net charge transfer within Fe–X–M superexchange interactions (M = transition metal and X = anion). We also pointed out the importance of the temperature dependence of the quadrupole splitting ($Q.S.$) as a criterion of localized versus itinerant electrons, and we showed that a temperature dependence occurs in intrinsically cubic fields if the minority-spin electron outside a closed majority spin half-filled shell of a high-spin Fe^{2+} ion is localized and Jahn–Teller-coupled to lattice vibrations to form vibronic states.

In this paper we consider the I.S. in more detail, demonstrating from available Mössbauer data that the I.S. for ^{57}Fe coordinated tetrahedrally or octahedrally by S^{2-} ions provides an excellent estimate of the number of minority-spin electrons per high-spin iron provided proper account is taken of any orbital degeneracy associated with itinerant minority-spin electrons. Data for proteins as well as for sulfides are considered.

In order to demonstrate the correlation between I.S. and mean formal valence state, it is necessary to refer to another

0022-4596/82/010001-22$02.00/0

paper (*2*), in which the relative energies of the $Fe^{2+}:3d^6$ level (or band) and the $S^{2-}:3p^6$ bands were explicitly considered for many of the compounds to be discussed in this paper. In summary, the $Fe^{2+}:3d^6$ level (or band) of tetrahedral-site iron was generally found to lie totally above the $S^{2-}:3p^6$ band edge as illustrated schematically in Fig. 1a, whereas the same level (or band) of octahedral-site iron more commonly appears to be just overlapped by the $S^{2-}:3p^6$ band as illustrated in Fig. 1b. Oxidation of a ferrous sulfide having no band overlap, as in Fig. 1a, introduces holes into the $Fe^{2+}:3d^6$ level only to create the formal valence state Fe^{3+}, but oxidation of a ferrous sulfide containing overlapping bands, as in Fig. 1b, may introduce mobile holes in the $S^{2-}:3p^6$ band as well as the $Fe^{2+}:3d^6$ level, which renders ambiguous the formal valence state of the iron. In this context, the term formal valence is used to designate the number of $3d$ electrons per iron atom. Where there are mixed valencies, the notation $Fe^{3+}_{1-x}Fe^{2+}_{x}$ will generally be used; however, where the minority-spin electrons are delocalized and hence shared commonly by more than one iron atom, the preferred notation is Fe^{m+} ($m = 3 - x$), and this will be used—but not exclusively—where this condition applies. If we can demonstrate that the Mössbauer I.S. gives a good measure of $\langle m+ \rangle$, then it is possible to deduce from the chemical formula the number of holes that must be present in any overlapping $S^{2-}:3p^6$ bands.

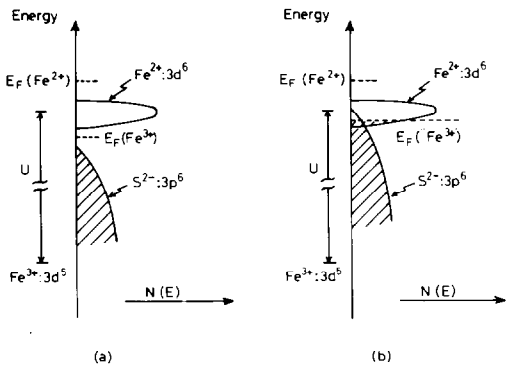

FIG. 1. Schematic energy versus density of electronic states for sulfides: (a) nonoverlap and (b) overlap of $S^{2-}:3p^6$ bands with minority-spin $Fe^{2+}:3d^6$ band separated an energy U from the majority-spin $3d^5$ configuration. Fermi energy E_F for ferrous and nominal ferric sulfide.

A second important emphasis in paper (*2*) was that the potential seen by the minority-spin electron of a high-spin Fe^{2+} ion is sufficiently different from that seen by the five majority-spin electrons, which are strongly stabilized by intraatomic exchange, that delocalization of a π-bonding minority-spin electron may occur where the σ-bonding majority-spin electrons are still localized. In particular, edge-shared tetrahedra and edge-shared octahedra containing high-spin iron were commonly found to have itinerant minority-spin electrons, and the character of the crystal structure was shown to be partially determined, in many cases, by the mean number of minority-spin electrons per high-spin iron ion—and hence by the formal valence. We will have occasion in this paper to reinforce this finding.

In Mössbauer spectroscopy, the isomer shift between the source A and an absorber B is proportional to the difference in charge density at the nucleus

$$\text{I.S.} \equiv \delta = a(|\psi_A(0)|^2 - |\psi_B(0)|^2), \quad (1)$$

where a is a calibration constant. The original calibration of a was carried out by Walker *et. al.* (*3*) from an analysis of Mössbauer data for ionic salts containing isolated ferrous and ferric ions. Their model used two independent charge-density terms:

$$|\psi(0)|^2_{\text{total}} = |\psi(0)|^2_{\text{ion}} + |\psi_{4s}(0)|^2, \quad (2)$$

where the first was the sum of the $1s$, $2s$, and $3s$ contributions for the free ion as estimated by Hartree–Fock calculations and the second was the $4s$ contribution, evaluated with the semiempirical Fermi–Segré

formula, arising from covalent back donation from the ligands to the iron ion. Where the Fe–Fe interactions are strong enough to delocalize all the $3d$ electrons or where the crystalline fields are strong enough to induce formation of a low-spin state, Eq. (2) must be modified by a correction term that takes into account changes in s-electron charge density at the nucleus due to changes in the extension of the $3d$ wavefunctions. Sawatzky and Van der Woude (*4*) have discussed these corrections and, in addition, included the distortion of the *ns* core-electron wavefunctions by the ligand electrons. All these ligand–iron interactions *increase* the charge density at the nucleus, thereby *reducing* the I.S. from the free-ion value. However, covalency involving charge transfer from the ligand to the $3d$ orbitals would seem to have an opposite effect were it not for a compensating influence from the attendant increase in the radial extension of the "*d*" orbitals with covalency. Although it is not yet clear whether the net contribution to the I.S. from d-orbital covalency is positive or negative, it is apparent empirically that, in total, covalency reduces the I.S.

In order to have some idea of the magnitude of this reduction for high-spin ions, it is instructive to compare the I.S. relative to metallic iron at 300 K for several ferrous and ferric halides and oxides. In the isostructural series FeX_2 (X = F, Cl, Br, and I), the room-temperature I.S. for the octahedral-site ferrous ions has the values 1.35, 1.10, 1.00, and 0.85 mm/sec, respectively (*5*). Values for the octahedral-site ferric ions in FeX_3 (X = F, Cl, Br) are 0.45, 0.35, and 0.20 mm/sec (*6*). Despite the marked change with electronegativity of the ligand, it is interesting that for a given ligand the range of I.S. values for a particular valence state and ligand coordination is small. Octahedral ferric ions in fluorides have an I.S. confined to the range $0.45 < \delta < 0.49$ mm/sec (*7, 8*), and in oxides to the range $0.35 < \delta < 0.44$ mm/sec, see Table I. In the garnet $Y_3Fe_5O_{12}$ (YIG), the I.S. at the tetrahedral (A-site) Fe^{3+} ions is considerably smaller, 0.20 mm/sec (average value between those reported in (*73*) and (*74*)) versus 0.39 mm/sec for the octahedral (B-site) Fe^{3+} ions. Such a reduction on changing from octahedral to tetrahedral coordination is to be expected; the metal–ligand distances are significantly shorter for tetrahedral coordination, and both covalency and core distortions are correspondingly larger. We will see that the mean I.S. for tetrahedral and octahedral high-spin "ferric" ions in sulfides are similar to those found in oxides, but are definitely smaller: 0.18 and 0.35 mm/sec, respectively. The same approximate increase of 0.17 mm/sec on going from tetrahedral to octahedral coordination is found.

It should be noted that the range of I.S. for a given coordination number, formal valence, and coordination anion may be enlarged by virtual superexchange charge transfer between the Fe atom and some other transition-metal atom M. Charge transfers to the Fe-atom $3d$ orbitals increase the I.S., those from the Fe-atom $3d$ orbitals decrease it.

The Isomer Shift in Mixed-Valency Sulfides

From the above discussion, we anticipate that high-spin iron ions in sulfides will have an I.S. for each valence state Fe^{m+} that differs little from a mean value $\bar{\delta}_{m+}$ provided superexchange charge transfers between Fe and an atom M are not too important. But in mixed-valency compounds, definition of the valency $m+$ may be difficult.

A mixed-valency compound is one in which an atom occupies similar crystallographic sites, but in more than one valence state. Magnetite, the ferrospinel $Fe^{3+}[Fe^{3+}Fe^{2+}]O_4$, is a famous example. At room temperature it is cubic, ferrimagnetic,

TABLE I

ROOM TEMPERATURE I.S. FOR OCTAHEDRAL Fe^{3+} IN OXIDES

Compound	α-Fe_2O_3	α-FeOOH	YIG	$CuFeO_2$	$LiFeO_2$	Fe_2TeO_4
I.S. (mm/sec)	0.37	0.35	0.39	0.39	0.35–0.40	0.44
Reference	*71*	*72*	*73, 74*	*49*	*50–52*	*82*

and a good electronic conductor. The minority-spin electrons move about on the octahedral B sites of this spinel via the charge-transfer reaction $Fe^{3+} + Fe^{2+} \rightarrow Fe^{2+} + Fe^{3+}$, and the time between electron transfers is short compared to the lifetime $\tau = 1.5 \times 10^{-7}$ sec of the ^{57}Fe excited state. Consequently only one octahedral-site resonance is observed at room temperature, and it has an I.S. that is midway between the values for Fe^{3+} and Fe^{2+} ions. In mixed-valency systems where the charge-transfer reaction is slow relative to the measurement time, as in K_xFeF_3, we may expect two octahedral-site spectra; one corresponds to Fe^{3+} and the other to Fe^{2+}. In such a system, the mean valence is given by the ratio of the intensities of the two separated Mössbauer spectra. In the case of fast electron transfer, on the other hand, the mean valence $\langle m+\rangle$ should be given by the isomer shift $\bar{\delta}_{\langle m+\rangle}$ of a single Mössbauer spectrum. If the magnitude of the I.S. varies linearly with valence state, we should have the room-temperature relation for high-spin iron

$$\bar{\delta}_{\langle m+\rangle} = A - B\langle m+\rangle, \qquad B \equiv (\bar{\delta}_{2+} - \bar{\delta}_{3+}), \quad (3)$$

where the constants A, and perhaps also B, depend on the anion coordination as well as the standard reference (taken herein as metallic iron at 300 K). This formula is, of course, precisely that given by Hoggins and Steinfink (*9*), who suggested the empirical relationship

$$\delta \text{ (in mm/sec)} = 1.4 - 0.4\langle m+\rangle \quad (4)$$

for high-spin iron tetrahedrally coordinated by sulphur. The particular numbers chosen for A and B in Eq. (3) depend on the values selected for $\bar{\delta}_{2+}$ and $\bar{\delta}_{3+}$. Hoggins and Steinfink chose $\bar{\delta}_{3+} = 0.20$ mm/sec and $\bar{\delta}_{2+} = 0.60$ mm/sec. In order to see whether such a relation is useful in the light of more experimental information, it is instructive first to reexamine $\bar{\delta}_{2+}$ and $\bar{\delta}_{3+}$ for various ferrous and ferric sulfides to determine $\bar{\delta}_{2+}$, $\bar{\delta}_{3+}$ and the extent of the range of I.S. about each mean value. Table II summarizes the Mössbauer data and some other properties of sulfides formally containing ferric ions for which iron Mössbauer data exist. Data for the ferrous sulfides have been summarized in (*1*).

Table IIIA lists the I.S. for several compounds selected from Table II containing Fe^{3+} ions in tetrahedral sites of sulfur. The range of values is only $0.18 < \delta_{3+}(\text{tet}) < 0.20$ mm/sec, the lowest occurring for $CsFeS_2$ and the highest for $CuFeS_2$. Although $AFeS_2$ (A = Cs, Rb, and K) consists of chains of edge-shared tetrahedra held together by A^+ ions and $CuFeS_2$, chalcopyrite, is an ordered tetragonal zincblende containing tetrahedral Cu^+ and Fe^{3+} ions on alternate (001) planes, the variation in δ_{3+}(tet) values is everywhere consistent with an increase in the electropositive character of the counter cation on going from Cu^+ to Cs^+; the covalent component of the Fe–S bond should increase as that component of the competing A–S bond decreases.

In Table IIIA, the room-temperature isomer shift for tetrahedral high-spin Fe^{2+} ions varies over a much larger range. The values for stannite, Cu_2FeSnS_4 with $\delta_{2+}(\text{tet}) = 0.44$

TABLE II

SOME PHYSICAL PROPERTIES OF SULFIDES FORMALLY CONTAINING FERRIC IONS FOR WHICH IRON MÖSSBAUER DATA EXIST

Compound	Mössbauer Data (300 K)				Other properties					
	I.S. (mm/sec)	$\epsilon = \Delta E/2$ (mm/sec)	H_{hf}(kOe) 300 K	H_{hf}(kOe) 4.2 K	Structure (300 K)	Electrical character	Magnetic order	T_N or T_C (K)	Comments	Ref.
1. $CsFeS_2$	0.18	0.21		150	rhombic		AF[a]	<77	Infinite chains of edge-shared Fe(III)S_4 tetrahedra	*16, 53*
2. $RbFeS_2$	0.19	0.22		196	monoclinic		AF[b]	185	idem	*16, 53*
3. $KFeS_2$	0.19	0.26		215	monoclinic	SC[c]	AF[d]	245	idem	*9, 16* *30, 53*
4. $NaFeS_2$	0.36	0.29		270			AF[e]	77		*15, 16*
5. $LiFeS_2$	0.40	0.35		470	—		AF[f]			*16*
6. $CuFeS_2$	0.23[g]	0.02[g]	356[g]	368[g]	chalcopyrite	SC[h]	AF[i]	823		*24 30–36*
	0.20	0.05	225	at 77 K						
	0.32	0.60		372						
	0.25	0								
7. $CuGaS_2$[j]	0.34	0.12			chalcopyrite	P-type SC	AF	<77	Spectrum obtained with 90% enriched ^{57}Fe, 6000 ppm concentration	*39*
8. $AgFe_2S_3$	0.38	0.5	267	274	unknown		AF[k]		Sternbergite	*36*
9. $CuFe_2S_3$[j]	0.22	0	0		cubic	SC				*30*
10. $CuFe_2S_3$	0.39[g]	0.26[g]	331	340	orthorhombic	SC[l]	AF[m]		cubanite	*30*
	0.42	0.60								*36, 40*
11. $BaFe_2S_3$	0.41	0.30			—	SC[n]				*11*
12. $BaVS_3$	0.45	0.68		220	hexagonal		AF	15	Stoichiometric, doped with 2% ^{57}Fe	*25*
13. $BaVS_{3-\delta}$	0.22	0.41		220	hexagonal		Ferro.	16	4% sulfur vacancies	*25*
14. Fe_2S_3	0.35 and 0.51 (at 78 K)	0.41 and 0.44		253	amorphous		AF		Two distinct Fe sites	*13*
15. Fe_3S_4[j]	0.26, 0.56	—	311		spinel	metal	Ferri.	606	Greigite	*27*
16. $Fe_{1.1}Cr_{1.9}S_4$	0.30	0.18			spinel				Nonstoichiometric compound	*26*
17. Cu_3FeS_4	0.53 (at 77 K)	0.03	0	350	tetragonal	p-type SC	AF[o]	76[p]	Bornite, low-temperature phase	*43*
18. CuV_2S_4	0.35				spinel	metal[q]	Pauli[r]		Doped with 5% ^{57}Fe, 90% enriched	*17, 75*
19. Ba_3FeS_5	0.17	0.25			—	SC[s]	AF[t]		Phase at 50 kbar and 1000°C	*24*
20. $Ba_{15}Fe_7S_{25}$	0.20	0.45	0		orthorhombic	SC[u]	AF[v]		Multisite Fe^{3+} compound	*24*

TABLE II—*Continued*

Compound	Mössbauer Data (300 K) I.S. (mm/sec)	$\epsilon = \Delta E/2$ (mm/sec)	H_{hf}(kOe) 300 K	H_{hf}(kOe) 4.2 K	Other properties Structure (300 K)	Electrical character	Magnetic order	T_N or T_C (K)	Comments	Ref.
21. $Ba_9Fe_{16}S_{32}$	0.20	0.32	0	248 (at 78 K) and 229	orthorhombic	SC[w]	AF		One Fe^{3+} site (doublet) at 300 K, two six-line Fe^{3+} sites at 78 K	*11*
22. $Ba_4Fe_2S_8$ $[S_{3/8}(S_2)_{4/8}]^x$	0.20 0.20	0.45 0.90	0		—	SC[u]	AF[x]		Two-site Fe^{3+} spectrum	*21*
23. $Ba_8[Ba_{0.6}Al_{0.4}]$ $Fe_2S_8[S_{0.6}$ $(S_2)_{0.4}]$	0.30	0.55	0		—			120	Multisite Fe^{3+} spectrum	*21*
24. $Ba_7Fe_6S_{14}$	0.49 0.36 0.36	0.80 0.65 0.35		from 200 to 295 (at 77 K)	—	SC[ab]	AF[ac]	200	Three-site Fe^{3+} spectrum	*22*
25. $Ba_6Fe_6S_{15}$	0.47	0.34	0	156 and 177 (at 78 K)	—	SC[ad]	AF[ae]		One paramagnetic doublet at 300 K, two six-line spectra at 78 K	*22*
26. Oxidized rubredoxin (Redox)	0.32 (powder) 0.25 (solution)	0.25		370 (at 77 K)	—				H_{hf} observed in Redox solution	*76, 77*
27. $(Et_4N)_2$ $[Fe_4S_4SCH_2Ph)_4]$	0.34[af]	0.57			—				One paramagnetic doublet spectrum	*78, 79*
28. $(Et_4N)_2$ $[Mo_2Fe_6S_8(SEt)_8]$	0.27 (at 77 K)	0.48			—					*47, 80*
29. $[(CH_2)_4N(S_2)]_2Fe$	0.40	0.18		430	—					*46*

Note. I.S. relative to metallic iron at 300 K, AF = antiferromagnetic, SC = semiconductor. See (*1*) and test for ferrous sulfides.

[a] Weak, temperature-independent paramagnetism, paramagnetic moment $\mu_{eff} = 4.38\ \mu_B$ (*53*).

[b] Weak, temperature-independent paramagnetism (*53*).

[c] Electrical resistivity $\rho = 10^3$ ohm-cm (*9*).

[d] Weak, temperature-independent paramagnetism, $\mu_{eff} = 4.61\ \mu_B$ (*53*).

[e] $\mu_{eff} = 4.65\ \mu_B$ (*16*).

[f] $\mu_{eff} = 4.68\mu_B$ (*53*).

[g] Values depending on the author.

[h] $\rho = 10^{-1}$ ohm-cm (*9*).

[i] Neutron diffraction moment at 300 K, $\mu_{Fe} = 3.85\ \mu_B$ (*35*). Magnetic susceptibility $\chi = 9.8.10^{-4}$ emu/mole (*34*).

[j] Presence of distinct Fe^{2+} and Fe^{3+} sites in this compound; only Fe^{3+} is given here. For Fe^{2+} see text and Ref. (*1*).

[k] Temperature-independent parmagnetism between 77 and 475 K; magnetic susceptibility $\chi = 2.10^{-6}$ emu/g (*36*).

[l] $\rho = 10$ ohm-cm (*9*).

[m] Neutron-diffraction atomic moment $\mu_{Fe} = 3.2\ \mu_B$; weak, spontaneous magnetism: $\mu_{Fe} = 0.042\ \mu_B$, $\mu_{Cu} = -0.00017\ \mu_B$ (*40*).
[n] $\rho = 0.5$ ohm-cm, $E_a = 0.16$ eV, paramagnetic moment $\mu_{eff} = 4.85\ \mu_B$ (*11*).
[o] Curie constant $C = 4.97$ emu K/mole, $\mu_{eff} = 6.3\ \mu_B$ (*43*).
[p] A second magnetic transition at 8 K was reported (*43*).
[q] Metallic between 300 and 120 K, SC at $T < 120$ K ($\rho = 6.5 \times 10^{-4}$ ohm-cm at 300 K) (*75*).
[r] Pauli paramagnetic at 90 K $\leq T \leq$ 300 K: $\chi = 1350 \times 10^{-6}$ emu/mole (*75*).
[s] $\rho = 10^5$ ohm-cm (*24*).
[t] $\mu_{eff} = 5.1\ \mu_B$ (*24*).
[u] High-resistivity S.C., $E_a = 0.5$ eV (*24*).
[v] $\mu_{eff} = 5.5\ \mu_B$ (*24*).
[w] $\rho = 1$ ohm-cm, $E_a = 0.14$ eV (*11*).
[z] Compounds with general formula $Ba_4(Ba_{1-x}Al_x)Fe_2S_8[S_{1-y}(S_2)_y]$ the first with $x = 0, y = \frac{1}{2}$ and the other with $x = 0.4$ and $y = 0.4$.
[y] $\rho = 10^5$ ohm-cm (*21*).
[z] $\mu_{eff} = 5.33\ \mu_B$ (*21*).
[ab] $\rho = 10^3$ ohm-cm, $E_a = 0.625$ eV (*21*).
[ac] $\mu_{eff} = 5.70\ \mu_B$ (*21*).
[ad] $\rho =$ ohm-cm, $E_a = 0.31$ eV (*21*).
[ae] $\mu_{eff} = 5.57\ \mu_B$ (*21*).
[af] Same I.S. for many complexes of the type $[(Fe_4S_4(SR)_4]^{2-}$. ΔE varies from 0.55 to 1.10 mm/sec (*79*).
[ag] Same I.S. for the molybdenum–iron–sulfur double-cubane cluster complexes $[MO_2Fe_6S(SC_2H_5)_9]^{3-}$ and $[MO_2Fe_6S_9(SC_2H_5)_8]^{3-}$ (*47, 80*).

mm/sec (*10*), and for $BaFe_2S_3$, with $\delta_{2+}(tet) = 0.41$ mm/sec (*11*), are clearly anomalous; the origin of these low values is discussed in the next paragraph. Of the remaining values for $\delta_{2+}(tet)$, the largest variation ($0.53 < \delta_{2+}(tet) < 0.77$ mm/sec) is found for the nominal normal spinels $Fe^{2+}[M_2^{3+}]S_4$ and $Fe_x^{2+}M_{1-x}'^{2+}[M_2^{3+}]S_4$. In these the Fe–S–$M$ interaction appears to play an unusually prominent role, and this problem is discussed in the next section. Elimination of the spinel data reduces the range of $\delta_{2+}(tet)$ for high-spin Fe^{2+} ions in tetrahedral sulfur coordination to $0.65 < \delta_{2+}(tet) < 0.70$ mm/sec. We therefore choose a $\bar{\delta}_{3+}(tet) \simeq 0.18$ mm/sec and a $\bar{\delta}_{2+}(tet) \simeq 0.68$ mm/sec to obtain from Eq. (3) the following relations for high-spin iron in tetrahedral sulfur coordination:

$$\bar{\delta}_{\langle m+\rangle} = 1.68 - 0.5\langle m+\rangle, \qquad (5)$$

where $\bar{\delta}_{\langle m+\rangle}$ is given in units of millimeters per second.

Let us now return to the anomalous $\delta_{2+}(tet) = 0.41$ and 0.44 mm/sec observed for $BaFe_2S_3$ and Cu_2FeSnS_4. The structure of $BaFe_2S_3$ is unusual (*12*); it contains linear double chains in which each tetrahedron shares three edges. As previously pointed out (*2*), this structural feature is apparently stabilized to allow the formation of three-electron Fe–Fe bonds perpendicular to the chain direction. In these three-electron bonds, a delocalized minority-spin electron does the bonding. In order for this to occur between tetrahedral-site Fe^{2+} ions, the π-bonding orbitals of e_g parentage must remain degenerate. Sharing the single minority-spin electron between two degenerate orbitals allows three-electron bonding in two perpendicular directions. But if such bonding occurs, we may anticipate that the minority-spin electron contributes to the I.S. as if it were delocalized into a three-electron bond, which means that the effective mean valence on the iron atom is $\langle m+\rangle = 2.5+$. From Eq. (5), an effective

TABLE III

ROOM TEMPERATURE I.S. FOR ^{57}Fe IN SULFIDES

$m = 3+$	*I.S.* [mm/sec]	Ref.	$m = 2+$	*I.S.* [mm/sec]	Ref.
		A. Tetrahedral Fe			
$CsFeS_2$	0.18	*16, 53*	ZnS : Fe	0.65,[a] 0.68[b]	*54, 55*
$RbFeS_2$	0.19	*16, 53*	CdS : Fe	0.70	*54, 55*
$KFeS_2$	0.19	*9, 16, 30, 53*	Ba_2FeS_3	0.62	*20*
$CuFeS_2$	0.20	*24, 30–36*	$BaFe_2S_3$	0.41	*11*
$Ba_4Fe_2S_6[S_{2/3}(S_2)_{1/3}]$	0.20	*21*	$Fe[Cr_2]S_4$	0.59	*28, 70*
			$Fe[RhCr]S_4$	0.60 (0.57)	*56* (*69*)
			$Fe[Sb_2]S_4$	0.62	*10*
			$Fe[Sc_2]S_4$	0.72	*57*
			$Fe[Nb_2]S_4$	0.77	*10*
			Cu_2FeGeS_4	0.64	*68*
			Cu_2FeSnS_4	0.44	*10*
		B. Octahedral Fe			
$NaFeS_2$	0.36	*15, 16*	$In[FeIn]S_4$	0.85 (0.80)	*58* (*10*)
$LiFeS_2$	0.40	*16*	FeS	0.83	*59–62*
CuV_2S_4 : Fe	0.35	*17*	Fe_2SiS_4[c]	0.82	*63*
			$FeMo_2S_4$	0.84	*64*
			FeV_4S_8	0.89	*65*
			$Fe_{0.56}Ta_2S_4$	0.83	*66*
			$FePS_3$	0.87	*67*

[a] Zincblende.
[b] Wurtzite.
[c] Olivine.

$\langle m+ \rangle = 2.5+$ gives a $\bar{\delta} \simeq 0.43$ mm/sec, which is close to the value (0.41 mm/sec) observed. A lowering of 0.02 mm/sec can be anticipated with a counter cation as electropositive as Ba^{2+}. From this example, it is clear that $\langle m+ \rangle$ in Eq. (5) must be considered an "effective" mean valence that can be increased by delocalization of the minority-spin electrons over degenerate e_g orbitals.

The structure of stannite, on the other hand, would seem to provide no such redefinition of $\langle m+ \rangle$. It consists of cation occupancy of corner-shared tetrahedral sites in a cubic-close-packed sulfur array, as in zincblende; but there is a distortion to tetragonal symmetry because of an ordering of Cu^+ ions on alternate (001) planes as in chalcopyrite, $CuFeS_2$. In stannite, the Fe^{3+} layers of chalcopyrite are replaced by ordered $Fe^{2+} + Sn^{4+}$ layers. However, the $Sn^{3+}: 5s^1$ and $Fe^{2+}: 3d^6$ bands are of comparable energy, so the Fe^{2+}-ion minority-spin electrons may occupy orbitals greatly extended by virtual charge transfers to the Sn^{4+} ions. A delocalization that creates a bandwidth for the minority-spin electrons that is greater than the tetragonal-field splitting of the orbitals of e_g parentage would distribute these "delocalized" electrons over two degenerate orbitals. An observed $\delta = 0.44$ mm/sec implies that the effective $\langle m+ \rangle$ at Fe^{2+} ions containing delocalized minority-spin electrons distributed over quasi-degenerate e_g orbitals is about 2.5+, corresponding to a half-electron contribution per Fe^{2+} ion to the I.S. from the minority-spin electrons. This observation reinforces the concept of an "effective" $\langle m+ \rangle$ applicable where the minority-spin elec-

trons at high-spin Fe^{2+} ions are distributed over quasi-degenerate orbitals. In contrast, isostructural Cu_2FeGeS_4 has a $\delta = 0.64$ mm/sec (*68*), characteristic of a normal Fe^{2+} ion with minority-spin e_g electrons confined to a single orbital of e_g parentage.

To obtain an empirical expression for octahedral-site iron is complicated by the possible overlap of the $Fe^{2+}: 3d^6$ and $S^{2-}: 3p^6$ bands as illustrated in Fig. 1b. This overlap makes it impossible to synthesize by high-temperature techniques a crystalline Fe_2S_3 because of the disproportionation reaction

$$Fe_2S_3 \rightarrow FeS + FeS_2, \qquad (6)$$

in which all of the holes in the two bands become concentrated in the antibonding states of the complex anion S_2^{2-}. However, an amorphous Fe_2S_3 has been stabilized, and its Mössbauer spectrum at 77 K exhibits two quadrupole doublets with I.S. = 0.35 and 0.51 mm/sec (*13*). Corrected to room temperature, these isomer shifts correspond approximately to 0.23 and 0.39 mm/sec, respectively. Although the local coordinations of the Fe^{3+} ions in this amorphous film were not determined, a quadrupole splitting indicates axial site symmetry for each iron site, and magnetic data indicate a high-spin state. These observations therefore suggest that the two quadrupole doublets represent distorted tetrahedral and octahedral sites, and this conjecture is reinforced by the report (*14*) of a ferrimagnetic Fe_2S_3 having the defect-spinel structure $Fe[\square_{1/3}Fe_{5/3}]S_4$ that was precipitated from an aqueous solution of $FeCl_3$ and $(NH_4)_2S$. However, rather than build on such a speculation, it is more prudent to look first (see Table IIIB) to the range $0.82 < \delta_{2+}(\text{oct}) < 0.89$ mm/sec of I.S. found with octahedral-site, high-spin Fe^{2+} ions. If the change from tetrahedral to octahedral coordination alters A, but not B, in Eq. (3), a $\bar{\delta}_{2+} \simeq 0.85$ mm/sec would give the room-temperature relation

$$\bar{\delta}_{\langle m+\rangle} \simeq 1.85 - 0.5\langle m+\rangle \qquad (7)$$

for high-spin iron in octahedral sulfur coordination, provided $\bar{\delta}_{\langle m+\rangle}$ is given in units of millimeters per second. Note that the change of 0.17 mm/sec on going from tetrahedral to octahedral coordination is just that observed for YIG. From Eq. (7), a $\bar{\delta}_{3+}(\text{oct}) \simeq 0.35$ mm/sec is predicted, which agrees well with the I.S. value 0.36 mm/sec reported for $NaFeS_2$ (*15*). Although the structure of the $NaFeS_2$ measured was not reported, we may assume it crystallized in the ordered-rocksalt structure with Na^+ and Fe^{3+} ions on alternate (111) planes as does $NaCrS_2$. Therefore a $\bar{\delta}_{3+}(\text{oct}) \simeq 0.35$ mm/sec indicates little overlap of the $Fe^{2+}: 3d^6$ level and the $S^{2-}: 3p^6$ band in this compound. In the case of $LiFeS_2$, which has an unknown structure, an I.S. of 0.40 mm/sec (*16*) would suggest that perhaps some overlap remains in this compound. The more electropositive the counter cation, the less likely is band overlap. A room-temperature I.S. of 0.35 mm/sec for the spinel CuV_2S_4 doped with 5 m/o iron 90% enriched with ^{57}Fe (*17*) points to Fe^{3+}-ion substitution on the octahedral B sites. In this case, a localized $Fe^{2+}: 3d^6$ level lies above the Fermi energy in overlapping $V^{3+}: 3d^2$ and $S^{2-}: 3p^6$ bands. Thus the data strongly support a $\bar{\delta}_{3+}(\text{oct}) \simeq 0.35$ mm/sec and the tentative assignment of the two resonances in amorphous Fe_2S_3 to tetrahedral and octahedral Fe^{3+} ions.

Applications

1. $AFeS_2$, $A = Cs, Rb, K, Na, Li$

The I.S. observed for each of these compounds was discussed above. The significant shift from 0.19 to 0.36 mm/sec on passing from $KFeS_2$ to $NaFeS_2$ has been attributed to a change from tetrahedral to octahedral coordination about the Fe^{3+} ions. Nevertheless, Taft (*15*) was able to demonstrate a linear relationship between

the hyperfine field H_{hf} acting at the iron nucleus and the electronegativity of the alkali ion for Cs, Rb, K, and Na. This correlation demonstrates that, for a fixed anion coordination, the hyperfine field, which varies from 150 kOe in $CsFeS_2$ to 215 kOe in $KFeS_2$ (see Table II), is much more sensitive to covalency than the I.S. The Fe–S covalency increases as the competing A–S covalency decreases; and the larger the Fe–S covalency, the smaller is H_{hf}. The simultaneous change of both H_{hf} and I.S. on passing from $KFeS_2$ to $NaFeS_2$ is, we suspect, largely due to a change in coordination of the Fe^{3+} ion from tetrahedral to octahedral. Therefore, the fact that H_{hf} for $NaFeS_2$ fits on the linear extrapolation of the $CsFeS_2$–$KFeS_2$ data may be fortuitous.

2. KLi_xFeS_2

The linear chains of edge-shared FeS_4 tetrahedra in $KFeS_2$ and the itinerant character of any minority-spin electrons added to these chains has suggested investigation of KLi_xFeS_2 as a battery-cathode material, the Li^+ ions intercalating between the chains and charge neutrality being maintained by a changing $\langle m+ \rangle$ for the iron chains (*18*). Moreover, Jacobson and McCandlish (*19*) have studied the Mössbauer spectrum of this system as a function of Li^+-ion insertion x. in an electrochemical cell. For $KFeS_2$ they found an I.S. in the range $0.17 < \delta_{3+}(\text{oct}) < 0.20$ mm/sec. The I.S. increased with x, but inhomogeneous Li^+-ion distribution rendered complex spectra. Nevertheless it was possible to identify resonances with an I.S. of 0.62 mm/sec in a fully discharged cell, which approaches a $\bar{\delta}_{2+}(\text{tet}) \simeq 0.68$ mm/sec. The authors discussed their results in terms of Eq. (4) and demonstrated that, with such an empirical relationship, useful information about such a system could be obtained from Mössbauer data.

3. *Ba–Fe–S Compounds*

A number of interesting ternary compounds have been synthesized within the Ba–Fe–S phase field, and the relationship between structure and $\langle m+ \rangle$ has been discussed (*2*). Moreover, it was shown above how an anomalous I.S. for tetrahedral Fe^{2+} ions in $BaFe_2S_3$ could be harmonized with these structural relationships. It is therefore of particular interest to see whether the Mössbauer data for the remaining compounds reveal additional insights.

Ba_2FeS_3 formally contains Fe^{2+} ions, and here the tetrahedra form linear chains of corner-shared tetrahedra rather than double chains of edge-shared tetrahedra as in $BaFe_2S_3$ (*12*). The magnetic susceptibility data indicated the presence of high-spin Fe^{2+} ions that experience a strong antiferromagnetic intrachain coupling, but a weak interchain coupling, and an I.S. of 0.65 mm/sec is typical for $\delta_{2+}(\text{tet})$ (*20*). With a very electropositive Ba^{2+} counter cation, a $\delta_{2+} < \bar{\delta}_{2+}$ is to be expected.

The compound $Ba_4Fe_2S_6[S_{2/3}(S_2)_{1/3}]$ contains only trivalent iron in two types of sites, isolated and paired tetrahedra; and the two types of iron have a common I.S. of 0.20 mm/sec, characteristic of $\delta_{3+}(\text{tet})$ (*21*). In fact, the exact value of $\langle m+ \rangle$ depends on the concentration of disulfide bonds as well as the Ba/Fe ratio, and an $\langle m+ \rangle = 2.97$ and 2.85 were estimated from bond distances for the isolated and paired iron, respectively. Substitution of Al^{3+} for Ba^{2+} in nearly isostructural $Ba_{3.6}Al_{0.4}Fe_2S_6[S_{0.6}(S_2)_{0.4}]$ introduces Al^{3+} ions into the Ba–S network, and the extra electron per Al^{3+} ion appears to reduce the paired ions. Again, from the bond distances $\langle m+ \rangle = 2.92$ and 2.63 are estimated for the two types of iron, and the Mössbauer spectrum was too complex to assign properly the I.S. and Q.S. associated with at least three types of resonances: isolated Fe^{3+}, paired Fe^{3+}, and paired $Fe^{2.5+}$. We would

anticipate an I.S. of about 0.42 mm/sec for the reduced pairs and 0.20 mm/sec for the Fe^{3+} ions; the spectrum is consistent with this assignment.

$Ba_7Fe_6S_{14}$ contains zig-zag linear chains composed of segments of three edge-shared tetrahedra that couple together by shared corners (*22*), and this chain-segment length has been shown to be consistent with the periodicity required to stabilize occupied, itinerant-electron states of minority-spin $3d$ electrons at the expense of the empty band states. Formally, each chain segment contains one hole in the Fe^{2+}: $3d^6$ band, and a critical question is the distribution of the minority-spin charge density. Although the compound is semiconducting, the analysis is based on the assumption that the minority-spin electrons are itinerant, as they are in all other cases where sulfur tetrahedra containing neighboring iron atoms share common edges. The structural refinement (*11, 22*) gives Fe_3–Fe_1–Fe_2 distances within a segment as 2.83 and 2.75 Å, respectively, indicating Fe_1–Fe_2 pairing. In addition, it shows an Fe_2–S_1–Fe_3 configuration that would optimize π-bonding over the S_1 atom with e_g orbitals perpendicular to the axis of the chain segment. Crudely, we could expect a charge distribution approaching Fe^{2+} + $2Fe^{2.5+}$ for each segment, and the structural data unambiguously indicates this would be distributed as $Fe_3^{2.5+}$–$Fe_1^{2.5+}$–Fe_2^{2+} rather than $Fe_3^{2.5+}$–Fe_1^{2+}–$Fe_2^{2.5+}$. Such a distribution is understandable if the π-bonding orbitals of the Fe_2–S_1–Fe_3 interaction are also delocalized, for now the Fe_2^{2+} ion is able to bond via two quasi-degenerate orbitals of e_g parentage exactly as do the Fe^{2+} ions in $BaFe_2S_3$. In fact, the structure now optimizes the possibility of forming three-electron bonds. As in $BaFe_2S_3$, the Fe_2^{2+} ion would then have an I.S. characteristic of $\langle m+\rangle = 2.5+$; and in $BaFe_2S_3$ a $\delta_{\langle 2.5+\rangle} \simeq$ 0.41 mm/sec was found. Consequently, the structural analysis predicts, after due account is taken of the orbital quasi-degeneracy on the Fe_2 ion, a $\bar{\delta} \simeq 0.41$ mm/sec with some differentiation between the three different types of iron ions. In fact, the Mössbauer data could be interpreted in two ways (*11*): (1) δ = 0.17, 0.39, 0.66 mm/sec, suggestive of Fe^{3+}, $Fe^{2.5+}$, and Fe^{2+}, or (2) δ = 0.36, 0.36, 0.49 mm/sec corresponding to a $\bar{\delta} \simeq 0.41$ mm/sec. The latter interpretation would seem to be preferred.

The basic structural unit of $Ba_6Fe_8S_{15}$ is an infinite columnar arrangement of FeS_4 tetrahedra consisting of a double-helical strand of edge-shared pairs connected by corners (*22*). A single quadrupole doublet with a room-temperature I.S. of 0.47 mm/sec (*11*) indicates delocalization of the two minority-spin orbitals of e_g parentage in this case also. Edge-shared pairing splits in two the orbital parallel to the columnar axis and stabilizes one minority-spin electron per iron pair in this orbital; within the pair, it creates the delocalized charge density of a three-electron Fe–Fe bond. The remaining 0.25 minority-spin electrons per iron atom are forced into the orbital of e_g parentage that is perpendicular to the columnar axis. If these remaining electrons were localized, we should predict an effective $\langle m+\rangle = 2.25+$, which would give a $\bar{\delta} \simeq$ 0.55 mm/sec. However, if all the minority-spin electrons are delocalized, then the remaining 0.25 minority-spin electrons per iron atom are equivalent to only half as much electronic density, and we predict an effective $\langle m+\rangle = 2.37+$ or a $\bar{\delta} \simeq 0.49$ mm/sec. With Ba^{2+} as the counter cation, the observed δ is consistently 0.02 mm/sec below the value predicted from Eq. (5), so again the π-bonding Fe–S–Fe interactions appear strong enough to delocalize the minority-spin electrons.

A preliminary structural investigation of nominal $Ba_9Fe_{16}S_{32}$ indicated (*11*) the presence of linear chains of edge-shared FeS_4 units as in $KFeS_2$; but these chains are held together by about half the number of Ba^{2+} ions as K^+ ions, so there is the possibility to

introduce "extra" Ba into the interstitial space to give $Ba_{8+x}Fe_{16}S_{32}$. The excess x Ba^{2+} ions per formula unit are charge compensated by $2x$ minority-spin electrons in the Fe–S chains. As itinerant electrons in the one-dimensional chains, the minority-spin electrons make the compound metallic parallel to the chain axis. As in the case of KLi_xFeS_2, the I.S. should provide a measure of the concentration $2x$ of itinerant electrons. From Eq. (5) we would predict a $\bar{\delta} = 1.68 - 0.5[3 - (x/8)] = [0.18 + (x/16)]$ mm/sec. The observed I.S. was 0.20 mm/sec (*11*). If 0.02 mm/sec is again subtracted from the empirical curve where Ba^{2+} is the counter cation, this observation would still correspond to $x = 0.64$ rather than the nominal $x = 1$ for $Ba_9Fe_{16}S_{32}$. If the I.S. value has an uncertainty of 0.02 mm/sec, then the nominal $x = 1$ falls within experimental error of the empirical formula (*5*), but the data do suggest that $x < 1$ is more probable. Subsequent structural work (*23*) has identified an infinitely adaptive series of compounds $Ba_p(Fe_2S_4)_q$ all containing the linear Fe–S chains and corresponding to the formula $Ba_{1+y}Fe_2S_4$ or $Ba_{8+x}Fe_{16}S_{32}$.

The compound $Ba_{15}Fe_7S_{25}$ (*24*) has a complex structure containing an isolated FeS_4 unit and two distinguishable trinuclear FeS_4 units. The two trinuclear units each consist of a central tetrahedron sharing a common edge with one terminal unit and a common corner with the other terminal unit. Thus there are seven inequivalent iron atoms in the unit cell, which makes difficult any analysis of the Mössbauer spectrum. The nominal formula corresponds to one minority-spin electron per seven inequivalent iron atoms; and we may anticipate its capture in one of the edge-shared pairs to give an I.S. of about 0.18 mm/sec for five iron atoms and about 0.41 mm/sec for two. Although the observed spectrum has been analyzed as consisting of seven quadrupole doublets having a common I.S. of 0.20 mm/sec, an alternate interpretation such as we suggest is possible, see Fig. 2.

Ba_3FeS_5 is a high-resistivity semiconductor containing isolated FeS_4 tetrahedra and, in its Mössbauer spectrum, having a single quadrupole doublet with an I.S. of 0.17 mm/sec at room temperature (*24*). These data pose an intriguing problem as the formal valence would correspond to Fe^{4+}, an impossible valence in a sulfide. In fact, the I.S. is that expected for an Fe^{3+} ion. But if the proper valence is Fe^{3+}, then there must be a hole in the sulfur $S^{2-}: 3p^6$ bands; and without the formation of identifiable S_2^{2-} complex anions in the structure, there is no apparent trap for the holes to keep the compound from being metallic. Moreover, magnetic susceptibility data (*24*) indicate an $S = 2$ spin state at the magnetic site. To reconcile the data, we are forced to the conclusion that the hole in the $S^{2-}: 3p^6$ bands is trapped within an FeS_4 complex and leaves a sulfur spin-$\frac{1}{2}$ coupled antiparallel to the $3d^5$ majority-spin configuration at the Fe^{3+} ion. The formal chemical formula could then be written $BaS \cdot Ba_2^{2+}[Fe^{3+}(S_4)^{7-}]$, where the $(FeS_4)^{4-}$ complex has a net spin $S = 2$, which satisfies the magnetic data, the iron has a high-spin $Fe^{3+}: 3d^5$ configuration, which satisfies the I.S., the $S^{2-}: 3p^6$ holes are trapped at isolated complexes, which satisfies the conductivity data, and there are no S_2^{2-} polyanions, which satisfies the structural data. Lemley *et al.* (*24*) remarked that the data require a "back-donation" of an electron from the sulfur to the iron, and the complex proposed is consistent with this idea. However, it explicitly back-donates a majority-spin electron from the sulfur ligands to the Fe: $3d$ orbitals to create an $Fe^{3+}: 3d^5$ configuration in a complex with a net spin $S = 2$.

The compound $BaVS_3$ contains linear chains of face-shared VS_6 octahedra, and doping with iron causes a substitution of low-spin iron for V^{4+} ions in stoichiometric

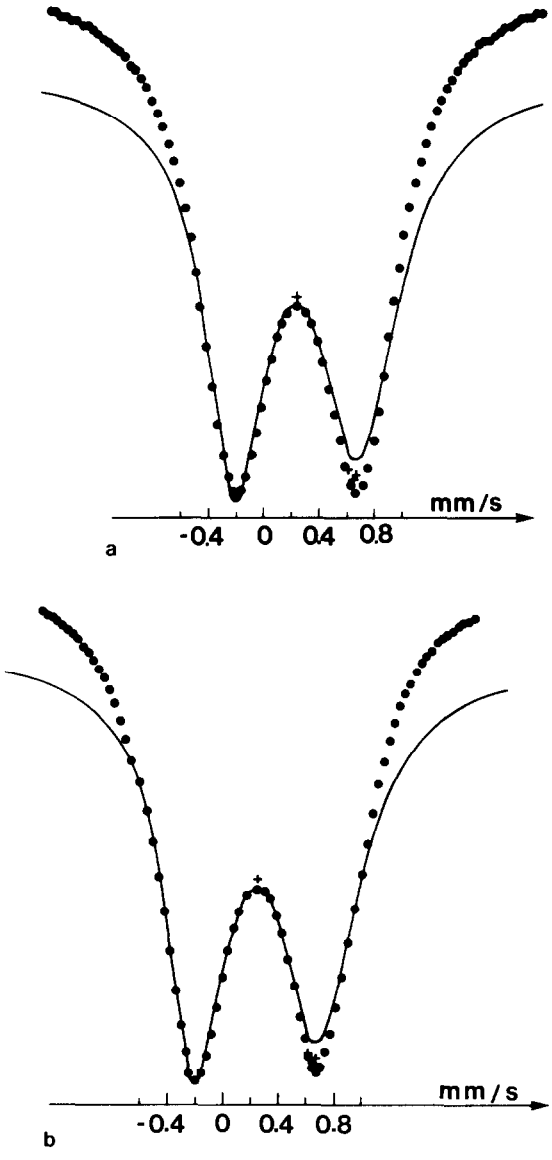

FIG. 2. Theoretical Mössbauer spectrum (black points) corresponding to seven overlapped ^{57}Fe quadrupole doublets: five with I.S. = 0.20 mm/sec and quadrupole splittings (a) ΔE = 0.75, 0.82, 0.93, 0.96, 1.04 mm/sec or (b) ΔE = 0.75, 0.82, 0.93, 1.00, 1.12 mm/sec, two with *I.S.* = 0.40 mm/sec and (a) ΔE = 0.85, 0.95 mm/sec or (b) ΔE = 0.89, 1.05 mm/sec. All lines for all sites were assigned Lorentzian lineshapes of equal relative intensity and linewidth (0.30 mm/sec at half-maximum); the assembly parameter was $\eta = 0$. The full line represents the fitting of Lemley *et al.* (*24*) to their data for $Ba_{15}Fe_7S_{25}$, and the crosses represent data points falling outside their fitting curve.

$BaVS_3$: Fe, but of high-spin Fe^{3+} for V^{4+} ions in 4% sulfur deficient $BaVS_3$: Fe (*25*). The I.S. for the Fe quadrupole doublet in the low-spin compound is 0.45 mm/sec, and in the sulfur-deficient compound it is 0.22 mm/sec. In the sulfur-deficient compound, the positive charge deficiency due to Fe^{3+} substitution for V^{4+} is accounted for by the sulfur vacancies; and it was assumed (*25*) that each sulfur vacancy attracts two Fe^{3+} ions to preserve local charge neutrality. Reduction of the high-spin Fe^{3+} coordination from six to five should result in an I.S. about half-way between that for six (0.35 mm/sec) and for four (0.17 mm/sec) coordination, giving a $\delta \simeq 0.26$ mm/sec. This estimate is somewhat higher than the observed value (0.22 mm/sec), which is more compatible with the I.S. for fourfold coordination. Since fivefold coordination is unusual for Fe^{3+} ions, it is possible that two bridging S^{2-} ions are removed from between the Fe^{3+}–Fe^{3+} pair to produce corner-shared tetrahedra. Charge compensation could be accomplished by either the loss of a Ba^{2+} ion or, more probably, the reduction of two adjacent vanadium ions to V^{3+}. In the stoichiometric compound, significant back donation from the S^{2-} ions to the empty e_g orbitals of low-spin, octahedral Fe atoms and from neighboring V^{4+} ions to the iron a_1 orbital of t_{2g} parentage would preserve charge neutrality while stabilizing a low effective charge on the iron. An I.S. of 0.45 mm/sec is distinctly higher than the 0.35 mm/sec anticipated for high-spin octahedral Fe^{3+} in a sulfide, which suggests that nearly two valence-band holes are created by a low-spin Fe substitution and that these holes are concentrated on neighboring VS_6 complexes.

4. Spinels

The inverse spinel $In[Fe_{1+x}In_{1-x}]S_4$ has an octahedral-site iron ion having a mean valence that decreases to 2+ as $x \to 0$. An I.S. varying from 0.80 to 0.85 mm/sec has

been reported for $FeIn_2S_4$, and we assume that the highest value approaches δ_{2+}(oct).

Doping of the normal spinel $Cu[V_2]S_4$ with Fe should substitute Fe^{3+} for vanadium to give $Cu[V_{2-\delta}Fe_\delta^{3+}]S_4$. Although the formal valence states of all the host atoms are ambiguous (*75*), we should expect that isolated iron ions will be stabilized in the Fe^{3+} state in this compound. In this case, the observed isomer shift corresponds to the predicted value, *viz.*, $\bar{\delta}_{3+}(\text{oct}) \simeq 0.35$ mm/sec.

The marked difference in δ_{2+}(tet) values observed for tetrahedral-site Fe^{2+} in spinels, see Table IIIA, is due to variations in the Fe^{2+}–S–M^{3+} interactions that are known to occur (*2*). In the system $Fe_{1-x}Co_x[Rh_2]S_4$, the M^{3+} ion is low-spin Rh(III): $t_{2g}^6e_g^0$; and in $Fe_{1-x}Cd_x[Cr_2]S_4$ it is Cr^{3+}: $t_{2g}^3e_g^0$. The characteristic feature of each system is strong S^{2-}–M^{3+} σ-bonding via empty e_g orbitals on the M^{3+} ions. This, in turn, causes a strong interaction with the t_{2g} orbitals of the A-site Fe^{2+}: $e_g^3t_{2g}^3$ ions, which also σ-bond with the S^{2-} ions. The result is a pronounced superexchange-type virtual charge transfer of t_{2g} electrons from A-site Fe^{2+} ions to the empty e_g orbitals of Rh(III) or Cr^{3+} ions; this charge transfer enhances the radial extension of the t_{2g} majority-spin electrons at the Fe^{2+} ions to such an extent that the quadrupole splitting is anomalously small. The virtual charge transfer also increases the effective $\langle m+\rangle$; an observed I.S. of 0.55 mm/sec would correspond to a virtual charge transfer approaching one-quarter of an electron per A-site iron. In the $Fe_xCd_{1-x}[Cr_2]S_4$ system, the I.S. apparently decreases with increasing x as $\bar{\delta}_{\text{tet}}(2+) = (0.60 - 0.08x)$ mm/sec in the range $0.02 \leq x \leq 0.75$ (*1*), which indicates an increasing tendency to delocalization of the minority-spin Fe^{2+} electrons with increasing iron concentration. On the other hand, $Fe[Cr_{2-x}Rh_x]S_4$ is reported (*70*) to exhibit a $\bar{\delta}_{\text{tet}}(2+) = (0.59 - 0.02x)$ mm/sec in the compositional range $0 < x <$ 1.2, again showing a tendency to greater delocalization of the minority-spin electrons with increasing numbers of Rh nearest neighbors.

The apparent discrepancy in the $Fe[Cr_2]S_4$ data relative to the extrapolation from the $Fe_xCd_{1-x}[Cr_2]S_4$ system probably reflects stoichiometry as well as data analysis. Brossard *et al.* (*26*) have studied nonstoichiometric $FeCr_2S_4$ annealed in both hydrogen and sulfur in order to identify the locations of the iron ions. In each sample, the room-temperature ^{57}Fe Mössbauer spectrum, which appeared as a broad singlet with $\delta \simeq 0.58$ mm/sec, was resolved into two singlets with $\delta \simeq 0.40$, 0.58 mm/sec and two quadrupole-split doublets with $\delta \simeq 0.56$, 0.62 mm/sec. The intensity of the $\delta \simeq 0.40$ singlet varied with the "Fe^{3+}" concentration and suggests the formation of tetrahedral-site Fe–Fe pairs, possibly associated with interstitial iron. The lack of any quadrupole splitting at the majority of the A-site Fe^{2+} ions indicates no dynamic Jahn–Teller distortion, which is consistent with a reduced I.S., $\delta \simeq 0.58$ mm/sec, due to extensive superexchange charge transfer to the Cr^{3+} ions.

In the case of $Fe[Sc_2]S_4$, the empty σ-bonding e_g orbitals at a Sc^{3+} ion are at too high an energy for significant charge transfer to occur. The situation is similar for the e_g orbitals of Nb^{3+} ions in $Fe[Nb_2]S_4$. Moreover, in this latter spinel any charge transfer will be from the Nb^{3+}: t_{2g}^2 ions to the empty e_g orbital of the Fe^{2+}: $e_g^3t_{2g}^3$ configuration, thereby reducing the effective $\langle m+\rangle$ on the Fe^{2+} ion and raising δ.

Greigite, the cubic-spinel form of Fe_3S_4, is a Néel ferrimagnet with a Curie temperature $T_c = 606$ K and a net molecular moment of $2.2 \pm 0.3\mu_B$ at 4.2 K (*27*), which is reduced because of a significant reduction of the atomic moments. Of particular interest is whether the reduction in the atomic moments is due to charge transfer from the S^{2-}: $3p^6$ valence band to the octahedral-site

Fe: $3d^6$ bands or to a delocalization of the iron $3d$ electrons that σ-bond to the sulfur. With a nominal formula $Fe^{3+}[Fe_2^{2.5+}]S_4$, we would expect a $\bar{\delta}$(tet) $\simeq$ 0.18 mm/sec and a $\bar{\delta}$(oct) $\simeq$ 0.6 mm/sec for localized majority-spin electrons on each subarray. In fact, a measured δ(tet) = 0.26 mm/sec and $\bar{\delta}$(oct) $\simeq$ 0.56 mm/sec suggests that little charge transfer from $S^{2-}: 3p^6$ to the $Fe^{2+}: 3d^6$ bands has taken place; rather a net superexchange charge transfer from B sites to A sites. Thus the Mössbauer data indicate that the nominal formula is more nearly $Fe^{2.84+}[Fe_2^{2.58+}]S_4$ and that the reduction in atomic moment as well as the fractional-valent nominal formula are due to a delocalization of the iron $3d$ electrons that σ-bond to the sulfur.

At this point, it is interesting to ask whether the Mössbauer data indicate the presence of holes in the $S^{2-}: 3p^6$ bands of metallic Fe_7S_8. The highest reported room-temperature I.S. for FeS is 0.83 mm/sec, close to that predicted from Eq. (7) for octahedral-site Fe^{2+} ions (*1*). In Fe_7S_8, the two values (for the distinguishable octahedral-site Fe atoms) fall in the range $0.65 < \delta < 0.69$ mm/sec. With an $\langle m+ \rangle = 16/7$, it follows from Eq. (7) that the I.S. for Fe_7S_8 should be about 0.15 mm/sec below that for FeS, which would give a value ($\delta \simeq 0.68$ mm/sec) falling in the observed range. Therefore there is no evidence for a significant concentration of broadband holes in Fe_7S_8; which is consistent with our conclusion about Fe_3S_4.

The spinel system $Fe^{2+}_{1-2x}Fe^{3+}_xCu^{+}_x[Cr_2]S_4$ should ideally be stable over the compositional range $0 < x < 0.5$, but the phase field has been found to extend to $x = 0.7$ (*28, 29*). Ando *et al.* (*69*) have recently measured, at 77 K, three compositions (x = 0.02, 0.14, 0.35) in this system. They analyzed their spectra on the basis of a stochastic model with two six-line spectra, corresponding to tetrahedral Fe^{2+} and Fe^{3+} ions, having an overlap that depends on the electron-transfer rate from Fe^{2+} to Fe^{3+} ions. The I.S. of both components decreased linearly with increasing x according to the relations $\delta_{tet}(2+) \simeq (0.72 - 0.3x)$ mm/sec and $\delta_{tet}(3+) \simeq (0.72 - 0.8x)$ mm/sec. For $x > 0.5$, they found evidence for only Fe^{3+}_{tet} with $\delta_{tet}(3+) = 0.32$ mm/sec, which corresponds well—on correcting for temperature—with a room-temperature $\delta_{tet}(3+) \simeq 0.20 \pm 0.01$ mm/sec previously reported by Haacke *et al.* (*28*) for $x = 0.7$. Such a finding implies that the $Fe^{2+}: 3d^6$ band is little overlapped by the broad $S^{2-}: 3p^6$ valence band, but that the valence band is able to tolerate a concentration of 0.2 holes per molecule before disproportionation to a stable $Cu[Cr_2]S_4$ spinel phase. This finding is of considerable interest in view of the continuing concern to define the nature of the holes in metallic, ferromagnetic $Cu[Cr_2]S_4$. Their definition is made difficult by an apparent overlap of $Cu^+: 3d^{10}$, $S^{2-}: 3p^6$, and $Cr^{3+}: 3d^3$ bands. We refer to the top of this band as $S^{2-}: 3p^6$; it appears that in $Fe_{1-x}Cu_x[Cr_2]S_4$ the top of this band has not been altered relative to the tetrahedral-site $Fe^{2+}: 3d^6$ level so as to allow significant overlap of the type shown in Fig. 1b. Such an alteration would have indicated the existence of Cu: $3d^{10}$ character at the top of the valence band.

5. *Other Sulfides Containing Copper*

Chalcopyrite, $CuFeS_2$, is a semiconductor with a tetragonal structure derived from zincblende; the Cu^+ and Fe^{3+} ions are ordered into alternate (001) planes of the corner-shared tetrahedral sites of zincblende. Although the I.S. reported for $CuFeS_2$ varies over the range $0.20 < \delta < 0.32$ mm/sec (*24, 30–36*), these several studies include mineral samples. Deviation from stoichiometry introduces divalent iron, which increases $\langle m+ \rangle$. A δ(tet) = 0.20 mm/sec is in good accord with that expected for a tetrahedral-site Fe^{3+} ion.

In $CuFeS_2$, the $S^{2-}: 3p^6$ band lies discretely below the empty $Fe^{2+}: 3d^6$ band as illustrated in Fig. 1a despite the presence of copper. This observation again indicates there is no important destabilization of the $S^{2-}: 3p^6$ band edge due to the $Cu^+: 3d^{10}$ core at tetrahedral site copper; therefore stabilization of holes in the valence band in $Cu[Cr_2]S_4$ and $Fe_{1-x}Cu_x[Cr_2]S_4$ for $0.5 < x < 0.7$ is probably due to a $Cr^{3+}: 3d^3$ level near the top of the $S^{2-}: 3p^6$ band as originally asserted by Lotgering and Van Stepele (*37*). However, given this situation, it is important to ask why the relative energies of the $Cr^{3+}: 3d^3$ and $Cu^+: 3d^{10}$ levels should have inverted on going from $Cu[Cr_2]O_4$, which contains Cu^{2+} and Cr^{3+} ions (*38*), to $Cu[Cr_2]S_4$. Clearly the increased covalent component of the bonding must be responsible. In the case of $Cu^+: 3d^{10}$, the $3d^{10}$ core is full and increased covalency involves only the $4s$, p orbitals. In the case of octahedral-site $Cr^{3+}: t_{2g}^3 e_g^0$, the empty e_g orbitals participate strongly in any covalent component of the bonding. An increased covalent charge transfer from the ligand to the metal ion will tend to increase the screening of the $3d$ electrons from the nuclear charge and hence to destabilize them. The much stronger covalence at the Cr^{3+} versus the Cu^+ ion, due to its larger charge as well as to the availability of empty σ-bonding $3d$ orbitals, means that on going from oxides to sulfides the $3d^3$ electrons at Cr^{3+} ions are destabilized to a greater extent than the $Cu^+: 3d^{10}$ electrons. It is this differential in destabilization that causes the crossover in the relative energies on going from the oxide to the sulfide. However, the fact that such a crossover occurs must mean that the $Cu^+: 3d^{10}$ core does not lie too far below the $Cr^{3+}: 3d^3$ level and the top of the $S^{2-}: 3p^6$ band in $Cu[Cr_2]S_4$.

The compound $CuGaS_2$ also crystallizes with the chalcopyrite structure, and iron doping produces two quadrupole doublets. One has a room-temperature I.S. of 0.75 mm/sec and is assigned to Fe^{2+}; the other has an I.S. of 0.34 mm/sec and is assigned to Fe^{3+} (*39*). The Fe^{2+}/Fe^{3+} ratio increased from about 0.01 in stoichiometric $CuGaS_2$ to 1.2 in a sample with 5 m/o Ga excess. In these doped samples, the irons are too far apart for fast electron transfer between them, so distinguishable valence states are observed. The systematic shift to higher I.S. values is suspicious, especially in view of an abnormally high Q.S. for Fe^{2+}_{tet} [see Table I of (*1*)]. At a doping level of only 6000 ppm, it is possible that the iron atoms occupy interstitial (octahedral) sites.

$CuFe_2S_3$ is polymorphic. A cubic phase contains copper and iron randomly distributed over the corner-shared tetrahedral sites of the zincblende structure, and its Mössbauer spectrum indicates localized, distinguishable Fe^{2+} and Fe^{3+} ions in the ratio $Fe^{2+}/Fe^{3+} = 1.15$ having a $\delta_{2+}(\text{tet}) = 0.72$ mm/sec and a $\delta_{3+}(\text{tet}) = 0.22$ mm/sec (*30*). Below 270°C, $CuFe_2S_3$ transforms to cubanite. In cubanite, the sulfur array is hexagonal-close-packed and the tetrahedral-site iron order so as to form pairs of edge-shared tetrahedra. As previously pointed out (*2*), this structural feature would be stabilized by the sharing of a minority-spin electron within each Fe–Fe pair. Such a model requires a common iron atomic moment, ferromagnetic coupling within a pair, and a single Mössbauer spectrum corresponding to $\langle m+ \rangle = 2.5+$, i.e., to a $\delta \simeq 0.44$ mm/sec. A single Mössbauer quadrupole doublet with $\delta \simeq 0.4$ mm/sec has been observed (*30, 36*). Neutron diffraction data have also revealed a single iron moment of $3.2\mu_B$ with ferromagnetic coupling of the Fe–Fe pairs, but antiferromagnetic coupling between the pairs (*40*). Thus the basic model of a shared minority-spin electron within each pair appears to be confirmed; the significant reduction in iron atomic moment is presumably due to a large antiparallel-spin charge transfer be-

tween antiferromagnetically coupled pairs via a superexchange interaction.

Sternbergite, $AgFe_2S_3$, is structurally less well characterized than cubanite, but again edge-shared pairs of tetrahedral-site iron can be expected. For this compound also a single Mössbauer quadrupole doublet has been observed; it has a $\delta = 0.38$ mm/sec, similar to that found in cubanite (*36*).

Cu_5FeS_4 is also characterized by several phases (*14, 42*). At high temperatures, the six cations are statistically distributed over the eight corner-shared tetrahedral sites of the fluorite structure. Below 500 K, the cations order among these sites; and below 423 K a complex phase called bornite is formed. Characterization of bornite has been made with magnetic, transport, and low-temperature Mössbauer measurements (*43*). It is an antiferromagnetic ($T_N = 76$ K), p-type semiconductor. However, the Mössbauer data below 79 K show two spectra, one of which has a smaller I.S. and belongs to a paramagnetic phase. The Mössbauer data suggest a spinodal decomposition below 423 K into a metal-poor, iron-rich phase $Cu_{5-3x+y}Fe_{1+x}S_4$ and a metal-rich, iron-poor phase $Cu_{5+3x-y}Fe_{1-x}S_4$. The iron-rich phase is antiferromagnetic; and the I.S., extrapolated to room temperature, is about 0.43 mm/sec. The volume of the paramagnetic phase decreases with decreasing temperature, suggestive of a range of magnetic-ordering temperatures, as should be expected if the spinodal disproportionation has not reached equilibrium. Since the I.S. of the antiferromagnetic phase suggests an $\langle m+ \rangle \simeq 2.5+$, we may assume a nearly 50–50 ratio of Fe^{2+} to Fe^{3+} ions in this phase, which fixes a $y = (1 + x)/2$ with $x > 0.2$. At $x = \frac{1}{3}$, the number of metal atoms in each phase is the same: $Cu_7Fe_2S_6$ and Cu_8FeS_6 having respective values of $\langle m+ \rangle = 2.5+$ and $3+$. Charge neutrality in the second phase is maintained by having an overlapping $S^{2-}: 3p^6$ band containing 1 hole per formula unit. At 4.2 K, the I.S. of the paramagnetic phase is about 0.21 mm/sec lower than the antiferromagnetic phase with an estimated $\langle m+ \rangle = 2.5+$, which is consistent with Fe^{3+} ions only. The I.S. of this phase anomalously increases with temperature for all $T < T_N$, and the resolution of the Mössbauer spectra appears to disappear as T approaches T_N. This observation suggests that spinodal decomposition has not reached equilibrium so that the volume of long-range magnetic order increases with decreasing temperature.

Although this model for bornite is speculative, the consistency with which the I.S. values could be interpreted in all the other sulfides provides confidence that the Mössbauer data is recording the existence of two phases, one of which has an $\langle m+ \rangle$ on tetrahedral-site iron that is near 2.5+. Reduction of the iron valence requires charge transfer from the Cu–S matrix and hence implicates a band overlap of the type illustrated in Fig. 1b. In this case, only copper is present to destabilize the $S^{2-}: 3p^6$ band, and it would appear that the greater the Cu/S ratio, the greater this destabilization.

6. *Proteins*

The nonheme iron–sulfur proteins active in metabolic processes contain one, two, four, or eight iron atoms. The one-iron proteins contain a single iron tetrahedrally coordinated with sulfur; these we should expect to give a Mössbauer spectrum characteristic of tetrahedral-site Fe^{3+} or Fe^{2+} with a $\bar{\delta}_{3+} \simeq 0.18$ mm/sec and a $\bar{\delta}_{2+} \simeq 0.68$ mm/sec. The two-iron proteins appear to consist of iron coordinated by edge-shared sulfur tetrahedra, so in this case three possible Mössbauer spectra can be imagined, one each for Fe_2^{2+} and Fe_2^{3+} with an I.S. similar to that for the one-iron proteins and a third $Fe_2^{2.5+}$ quadrupole-split spectrum with an I.S. midway between these two extremes ($\bar{\delta} \simeq 0.44$ mm/sec). The four-iron and eight-iron proteins contain

one or two Fe_4S_8 clusters of iron in sulfur tetrahedra that share three common edges with each other, see Fig. 3a. This unit allows Fe–Fe bonding via minority-spin $3d$ electrons on the iron to occur via both e_g orbitals so long as the e_g orbitals remain degenerate, and the Fe–Fe distances in the clusters are comparable to those in sulfides where delocalization of the minority-spin electrons is found. However, structural refinement of complexes $[Fe_4S_4(SR)_4]^{n-}$, where $n = 2$ or 3, have demonstrated the existence of Jahn–Teller deformations of the structure that remove the e_g-orbital degeneracy (*44*). Therefore the effective $\langle m+ \rangle$ should approach that predicted from simple electron population: $\langle m+ \rangle = 3+$ for Fe_4^{3+}, 2.75+ for $Fe_3^{3+}Fe^{2+}$, 2.5+ for $Fe_2^{3+}Fe_2^{2+}$, 2.25+ for $Fe^{3+}Fe_3^{2+}$, and 2+ for Fe_4^{2+}. Moreover, a series of complexes containing different R groups and different ionization $n-$ have been prepared (excluding an example of $Fe_3^{3+}Fe^{2+}$) for comparison with the properties of natural proteins in four different oxidation states. The Mössbauer data have been summarized (*44*), and it is instructive to compare the isomer shifts at 77K relative to metallic iron for (a) the complexes, δ_c, (b) the prediction from Eq. (5), $\bar{\delta}$, and (c) the proteins, δ_p.

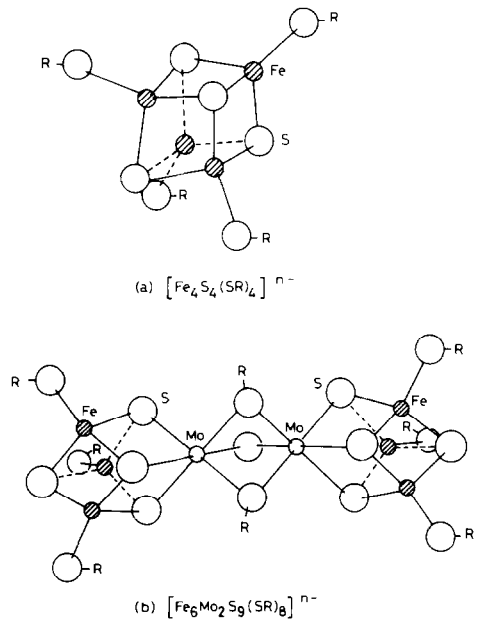

FIG. 3. Fe–S and Fe–Mo–S units in complexes and proteins.

	$\langle m+ \rangle$	δ_c(77K)	$\bar{\delta}$(R.T.)	δ_p(77K) (mm/sec)
Fe_4^{3+}	3+	0.13–0.17	0.18	0.25
$Fe_3^{3+}Fe^{2+}$	2.75+	—	0.31	0.32
$Fe_2^{3+}Fe_2^{2+}$	2.5+	0.35	0.44	0.43
$Fe^{3+}Fe_3^{2+}$	2.25+	0.56–0.61	0.56	0.57–0.59
Fe_4^{2+}	2+	0.61–0.64	0.68	0.60–0.65

Except for the nominally trianion complexes containing $Fe^{3+}Fe_3^{2+}$, which showed two quadrupole doublets of nearly equal intensity, the Mössbauer spectra were all single quadrupole doublets. It may be suspected that the exception contains a mixture of $Fe^{3+}Fe_3^{2+}$ and Fe_4^{2+} units. Since the variation in δ between 77 K and room temperature appeared to be small, the general agreement between observation and Eq. (5) is quite striking. These data are also consistent with Mössbauer data for one-iron complexes, which gave $\delta_c(77\text{ K}) = 0.13$ and 0.61 mm/sec for Fe^{3+} and Fe^{2+}, respectively (*45*).

The ^{57}Fe Mössbauer spectra of Fe^{3+} ions octahedrally coordinated by sulfur in complexes of the type $[(RR'NCS_2)_3Fe]^{n-}$ have been taken in an attempt to monitor high-spin/low-spin crossover (*46*). The room-temperature I.S. for a high-spin complex was $\delta = 0.40$ mm/sec, which is to be compared with a $\bar{\delta}_{2+}(\text{oct}) \simeq 0.35$ mm/sec predicted from Eq. (7). Thus here also the principal contribution to the I.S. appears to come from the nearest-neighbor atom, so the empirical formula provides a fair guide to the valence state of the iron atom. Interestingly, the complexes containing a reasonable fraction of low-spin state had an I.S. that was not perceptibly different from that of the high-spin state.

As a final example, the complex $[Mo_2Fe_6S_8(SEt)_9]^{3-}$ contains a large cluster consisting of two Fe_3Mo units in place of an Fe_4 unit, the two Mo ions being connected by three bridging S or SR ligands to place the Mo in face-shared sulfur octahedra, see Fig. 3b. The six iron atoms are coordinated tetrahedrally by sulfur, and an $\langle m+\rangle = \frac{8}{3}$ is expected to give a single quadrupole doublet with, from Eq. (5), a $\bar{\delta} = 0.35$ mm/sec. In the absence of a Jahn–Teller deformation, an effective $\langle m+\rangle = \frac{17}{6}$ would give $\bar{\delta} = 0.27$ mm/sec. At 77 K, the measured I.S. is $\delta_c(77\ K) = 0.27$ mm/sec (*80*).

Conclusions

This paper has refined the empirical formula of Hoggins and Steinfink [9], Eq. (4), in three ways: (1) More extensive empirical information was used to obtain Eq. (5) for high-spin iron tetrahedrally coordinated to sulfur. (2) An analogous empirical formula was developed for iron octahedrally coordinated by sulfur. (3) Definition of the effective valence $\langle m+\rangle$ was extended to include not only delocalization of the minority-spin electrons in the presence of localized (or strongly correlated) majority-spin electrons, but also the effect of orbital degeneracy. Figure 4 demonstrates that the I.S. is sensitive to nearest-neighbor anion coordination, but is much less sensitive than the hyperfine field H_{hf} to the character of the competitive bonding with these anions, as can be seen by comparing H_{hf} for Fe^{3+}_{tet} in compounds No. 1, 2, 3, and 21 of Table 2 or for Fe^{3+}_{oct} in compounds No. 4, 5, and 24 of Table 2. However, it is not insensitive to virtual charge transfer to neighboring cations via Fe–S–*M* superexchange interactions.

Application of the empirical formulae has established their usefulness for the following purposes:

(1) The rate of minority-spin charge transfer relative to the lifetime of the ^{57}Fe excited state allows a measure of the Fe–Fe bonding via delocalization of these electrons. It also establishes the proposition (*48*) that localized α-spin and delocalized β-spin electrons can coexist on the same atom.

(2) The direction of the net charge transfer in an Fe–S–*M* superexchange interaction can be determined, as was illustrated by the discussion on spinels.

(3) The detailed character of the Fe–Fe bonding could be established through a measure of $\langle m+\rangle$ and a knowledge of the chemical composition and structure, as was illustrated from the discussion of several barium–iron sulfides. In fact, delocalization of minority-spin electrons was shown to result from Fe–S–Fe π bonding as well as from direct Fe–Fe bonding.

(4) Changes in $\langle m+\rangle$ with cation intercalation can be monitored as illustrated by the insertion-electrode material KLi_xFeS_2 and the infinitely adaptive structure $Ba_{1+x}Fe_2S_4$.

(5) The sulfur coordination of iron can be assessed where structures are unknown, as illustrated by amorphous Fe_2O_3, $NaFeS_2$, and $LiFeS_2$, or where iron is used as a probe, as in $BaVS_3$: Fe.

(6) From an empirical $\langle m+\rangle$, it is possito to determine whether the formal valence state reflects a measure of the Fe : $3d^6$ population and to estimate the extent of any hole population in an overlapping S^{2-} : $3p^6$ band. This latter situation was illustrated in Ba_3FeS_5, Fe_3S_4, $Fe_{1-x}Cu_x[Cr_2]S_4$, $Fe_{1-x}S$, and bornite.

(7) The formal valence state of iron–sulfur units in complexes and proteins can be estimated from the same empirical formula used for sulfides, but some ambiguity arises from the dependence of $\langle m+\rangle$ on whether a cooperative Jahn–Teller deformation of the cluster has occurred. Superexchange charge transfer between cluster and ligands can also shift the δ versus $\langle m+\rangle$ line from the empirical formula by nearly as much as

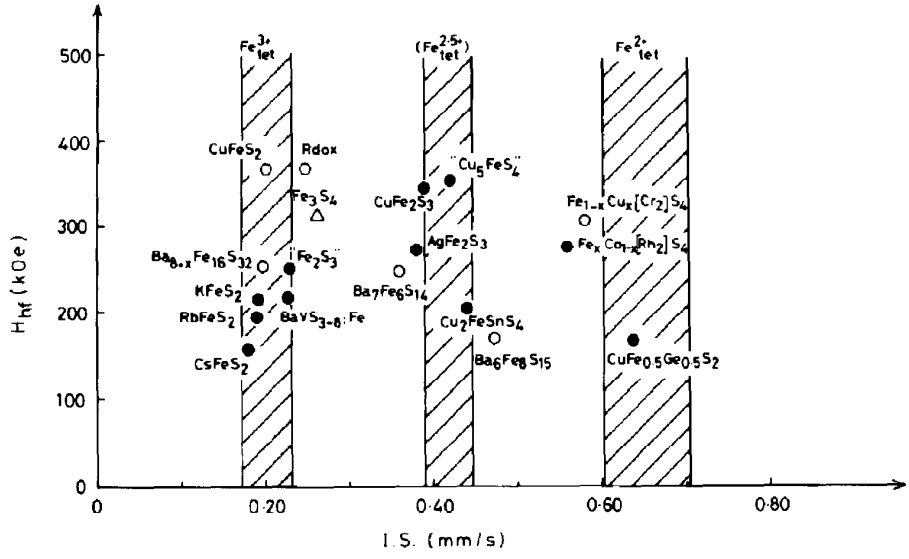

(a) Tetrahedral Iron.

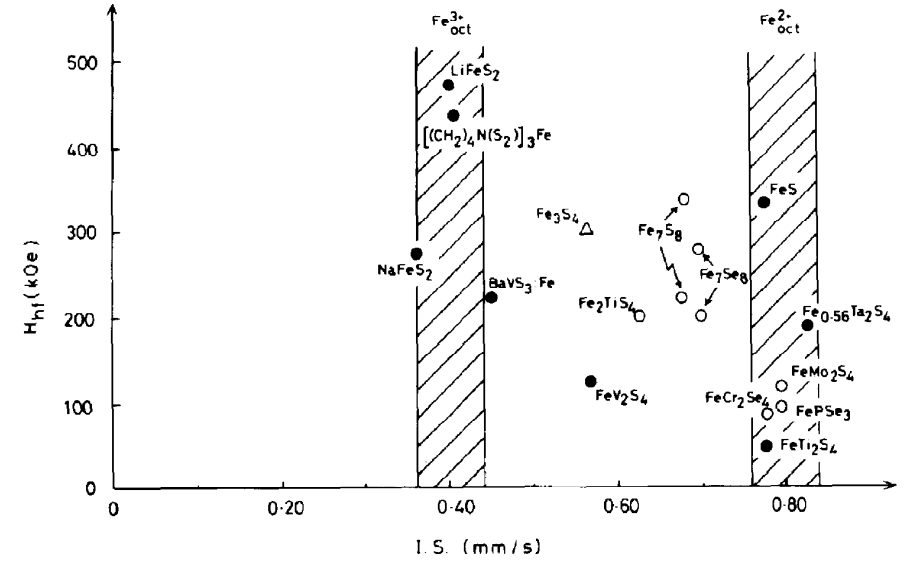

(b) Octahedral Iron.

FIG. 4. Hyperfine field H_{hf} at 4.2 (●), 77 (○), or 300 K (△) versus I.S. at 300 K. Data taken from Table II or Table I of Ref. (*1*); for Cu_2FeSnS_4 (*81*), $CuFe_{0.5}Ge_{0.5}S_2$ (*68*).

do the oxidation steps of a larger cluster. The data suggest the ligands on the complexes are electron acceptors whereas in the proteins they donate electrons to Fe^{3+} ions.

References

1. G. A. FATSEAS AND J. B. GOODENOUGH, *J. Solid State Chem.* **33,** 219 (1980).
2. J. B. GOODENOUGH, *Mater. Res. Bull.* **13,** 1305 (1978).
3. L. R. WALKER, G. K. WERTHEIM, AND V. JACCARINO, *Phys. Rev. Lett.* **6,** 98 (1961).
4. G. A. SAWATZKY AND F. VAN DER WUNDE, *J. Phys. (Paris)* **75,** C6-47 (1974).
5. F. VARRET, *J. Phys. (Paris)* **37,** C6-437 (1976).
6. J. DANON, "Applications of the Mössbauer effect in Chemistry and Solid State Physics," p. 100. Techn. Reports, Series No. 50 Intern. At. Energy Agency, Vienna, 1966.
7. N. N. GREENWOOD, F. MENIL AND A. TRESSAUD, *J. Solid State Chem.* **5,** 402 (1972).
8. J. M. DANCE, R. SABATIER, F. MENIL, M. WINTENBERGER, J. C. COUSSEINS, G. LE FLEM, AND A. TRESSAUD, *Solid State Commun.* **19,** 1059 (1976).
9. J. T. HOGGINS AND H. STEINFINK, *Inorg. Chem.* **15,** 1682 (1976).
10. M. EIBSHUTZ, E. HERMON AND S. SHTRIKMAN, *J. Phys. Chem. Solids* **28,** 1633 (1967).
11. W. M. REIFF, I. E. GREY, A. FAN, Z. ELIEZER, AND H. STEINFINK, *J. Solid State Chem.* **13,** 32 (1975).
12. H. HONG AND H. STEINFINK, *J. Solid State Chem.* **5,** 93 (1972).
13. A. H. STILLER, B. J. MCCORMICK, P. RUSSELL, AND P. A. MONTANO, *J. Amer. Chem. Soc.* **100,** 2554 (1978).
14. S. YAMAGUCHI AND H. WADA, *J. Appl. Phys.* **44,** 1929 (1973).
15. C. A. TAFT, *J. Phys. (Paris)* **38,** 1161 (1977).
16. C. A. TAFT, S. T. DA CUNHA, N. G. DE SOUZA, AND N. C. FURTADO, *J. Phys. Chem. Solids* **41,** 61 (1980).
17. G. A. FATSEAS, unpublished results.
18. A. J. JACOBSON, M. S. WHITTINGHAM, AND S. M. RICH, *J. Electrochem. Soc.* **126,** June (1979).
19. A. J. JACOBSON AND L. E. MCCANDLISH, *J. Solid State Chem.* **29,** 355 (1979).
20. N. NAKAYAMA, K. KASUGE, S. KACHIS, T. SHINJO, AND T. TAKADA, *J. Solid State Chem.* **33,** 351 (1980).
21. J. T. HOGGINS, L. E. RENDON-DIAMIRON, AND H. STEINFINK, *J. Solid State Chem.* **21,** 79 (1977).
22. I. E. GREY, H. HONG, AND H. STEINFINK, *Inorg. Chem.* **10,** 340 (1971).
23. J. S. SWINNEA AND H. STEINFINK, *J. Solid State Chem.* **32,** 329 (1980).
24. J. T. LEMLEY, J. M. JENKS, J. T. HOGGINS, Z. ELIEZER, AND H. STEINFINK, *J. Solid State Chem.* **16,** 117 (1976).
25. O. MASSENET, J. MERCIER, A. CHANG, R. BADER, AND A. B. H. MOHAMED, *J. Phys. Chem. Solids* **41,** 1009 (1980).
26. L. BROSSARD, L. GOLDSTEIN, P. GIBART, AND J-L. DORMAN, *J. Phys. Chem. Solids* **41,** 669 (1980).
27. M. R. SPENDER, J. M. D. COEY, AND A. H. MORRISH, *Canad. Phys.* **50,** 2313 (1972).
28. G. HAACKE AND A. J. NOJIC, *Solid State Commun.* **6,** 363 (1968).
29. F. K. LOTGERING, R. P. VAN STAPELE, G. H. A. M. VAN DER STEEN, AND J. S. VAN WIERINGEN, *J. Phys. Chem. Solids* **30,** 799 (1969).
30. N. N. GREENWOOD AND H. J. WHITFIELD, *J. Chem. Soc. A.*, 1697 (1968).
31. D. RAJ, K. CHANDRA, AND S. P. PURI, *J. Phys. Soc. Japan,* **24,** 39 (1968).
32. F. ARAMU, T. BRESSANI, AND P. MANCA, *Nuovo Cimento B* **51,** 370 (1967).
33. T. TERANICHI, *J. Phys. Soc. Japan* **16,** 1881 (1961).
34. R. ADAMS, P. RUSSO, R. ARNOTT, AND A. WOLD, *Mater. Res. Bull.* **7,** 93 (1972).
35. G. DONNAY, L. M. CORLISS, J. D. H. DONNAY, N. ELLIOT, AND J. M. HASTINGS, *Phys. Rev.* **112,** 1917 (1958).
36. P. IMBERT AND M. WINTENBERGER, *Bull. Soc. Mineral Cristallogr.* **90,** 299 (1967).
37. F. K. LOTGERING AND R. P. VAN STAPELE, *Solid State Commun.* **5,** 143 (1967).
38. E. PRINCE, *Acta Crystallogr.* **10,** 554 (1957).
39. H. J. VON BARDLEBEN, A. GALTZÉNÉ, C. SCHWAB, J. M. FRIEDT, AND R. POINSAT, *J. Appl. Phys.* **46,** 1736 (1975).
40. M. WINTENBERGER AND A. DELAPALME, *in* "Extended Abstracts, Intern. Conv. Solid Compounds of Transition Elements (Uppsala, June 21–25, 1976)," p. 132.
41. N. MORIMOTO, *Acta Crystallogr.* **17,** 351 (1964).
42. G. ALLAIS AND J. C. R. WYART, *C.R. Acad. Sci. Paris* **260,** 6583 (1965).
43. M. G. TOWNSEND, J. R. GOSSELIN, R. J. TRUNTLAY, L. G. RIPLEY, D. W. CARSON, AND W. B. MUIR, *J. Phys. Chem. Solids* **38,** 1153 (1977).
44. E. J. LASKOWSKI, R. B. FRANKEL, W. O. GILLAM, G. C. PAPAEFTHYMION, J. RENAUD, J. A.

IBERS, AND R. H. HOLM, *J. Amer. Chem. Soc.* **100,** 5322 (1978).
45. R. W. LANE, J. A. IBERS, R. B. FRANKEL, G. C. PAPAEFTHYMION, AND R. H. HOLM, *J. Amer. Chem. Soc.* **99,** 84 (1977).
46. R. RICHARDS, C. E. JOHNSON, AND H. A. O. HILL, *J. Chem. Phys.* **48,** 5231 (1968).
47. T. E. WOLF, J. M. BERG, P. P. POWER, K. O. HODGSON, AND R. HOLM, *Inorg. Chem.* **19,** 430 (1980).
48. J. B. GOODENOUGH, *Mater. Res. Bull.* **6,** 967 (1976).
49. A. H. MUIR, JR. AND H. WIDERSICH, *J. Phys. Chem. Solids* **28,** 65 (1967).
50. D. E. COX, G. SHIRANE, P. A. FLINON, S. L. RUBY, AND W. J. TAKEI, *Phys. Rev.* **132,** 1547 (1963).
51. N. RAMACHANDRAN AND A. B. BISWAS, *J. Solid State Chem.* **30,** 61 (1979).
52. G. A. FATSEAS AND S. LEFEBVRE, *C.R. Acad. Sci. (Paris) B* **266,** 374 (1968).
53. W. BRONGER, P. MÜLLER, AND D. SCHMITZ, *in* "Proceedings, Second Int. Conf. on Transition Elements (Enschede, June 12–16)" (1967).
54. A. GERARD, P. IMBERT, H. PRANGE, F. VANET, AND M. WINTENBERGER, *J. Phys. Chem. Solids* **32,** 2091 (1971).
55. G. GARCIN, P. IMBERT, AND G. JEHANO, *Solid State Commun.* **21,** 545 (1977).
56. H. KONDO, *J. Phys. Soc. Japan* **41,** 1247 (1976).
57. L. BROSSARD, H. OUDET, AND P. GIBART, *J. Phys. (Paris)* **37,** C6-23 (1976).
58. L. BROSSARD, L. GOLDSTEIN, AND M. GUITARD, *J. Phys. (Paris)* **37,** C6-493 (1976).
59. G. N. GONCHAROV, YU. M. OSTANEVICH, S. B. T. MILOV, AND L. CSER, *Phys. Status Solidi* **37,** 141 (1970).
60. H. HORITA AND E. HIRAHARA, *Sci. Rep. Tohoku Univ. Ser. I* **54,** 127 (1971).
61. S. ANZAI AND K. OZAWA, *Phys. Status Solidi A* **24,** K31 (1974).
62. J. L. HORWOOD, M. G. TOWNSEND, AND A. H. WEBSTER, *J. Solid State Chem.* **17,** 35 (1976).
63. C. MEYER, Y. GROS, H. VINCENT, AND E. F. BERTAUT, *J. Phys. Chem. Solids* **37,** 1153 (1976).
64. G. A. FATSEAS, J. L. MEURY, AND F. VARRET, *J. Phys. Chem. Solids* **42,** 239 (1981).
65. Y. OKA, K. JOSUGE, AND S. KACHI, *Mater. Res. Bull.* **12,** 1117 (1977).
66. M. EIBSHUTZ, F. J. DI SALVO, G. W. HULL, JR., AND S. MAHAJAN, *Appl. Phys. Lett.* **27,** 464 (1975).
67. B. E. TAYLOR, J. STEGER, AND A. WOLD, JR., *Solid State Chem.* **7,** 461 (1973).
68. P. IMBERT, F. VARRET, AND M. WINTENBERGER, *J. Phys. Chem. Solids* **34,** 1675 (1973).
69. K. ANDO AND Y. NISHIARA, *J. Phys. Chem. Solids* **41,** 1273 (1980).
70. E. RIEDEL AND R. KARL, *J. Solid State Chem.* **35,** 77 (1980).
71. O. C. KISTNER AND A. W. SUNYAR, *Phys. Rev. Lett.* **4,** 412 (1960).
72. J. B. FORSYTH, I. G. HEDLEY AND C. E. JOHNSON, *J. Phys. C.* **1,** 179 (1968).
73. L. BROSSARD, R. KRISHNAN, AND G. A. FATSEAS, *in* "Proceedings, Intern. Conf. Mössbauer Spectrosc. (Tihany June 1969)" (Academiai, Ed.). Kiado, Budapest, (1971).
74. J. NICHOLSON AND G. BURNS, *Phys. Rev.* **133**(6A), 1568A (1964).
75. N. LE NAGARD, A. KATTY, G. COLLIN, O. GOROCHOV, AND A. WILLIG, *J. Solid State Chem.* **27,** 267 (1979).
76. C. SCHULZ AND P. G. DEBRUNER, *J. Phys. Colloq. 6* **37,** 153 (1976).
77. R. B. FRANKEL, G-C. PAPAEFTHYMION, R. W. LANE, AND R. H. HOLM, *J. Phys. Colloq. 6* **37,** 165 (1976).
78. R. H. HOLM, B. A. AVERILL, J. HERSKOVITZ, R. B. FRANKEL, H. B. GRAY, O. SIIMAN, AND F. J. GRUNTHANER, *J. Amer. Chem. Soc.* **96,** 2644 (1974).
79. R. B. FRANKEL, B. A. AVERILL, AND R. H. HOLM, *J. Phys. Colloq. 6* **35,** 107 (1974).
80. T. E. WOLF, J. M. BERG, K. O. HODGSON, R. B. FRANKEL, AND R. H. HOLM, *J. Amer. Chem. Soc.* **101,** 4140 (1979).
81. U. GANIEL, E. HERMON, AND S. SHTRIKMAN, *J. Phys. Chem. Solids* **33,** 1873 (1972).
82. T. BIRCHALL, *J. Solid State Chem.* **27,** 293 (1979).